Published in final edited form as:
Am J Orthod Dentofacial Orthop. 2009 September ; 136(3): 312.e1–313. doi:10.1016/j.ajodo.2008.12.018.

Precision of cephalometric landmark identification: Cone-beam computed tomography vs conventional cephalometric views

John B. Ludlow[a], **Maritzabel Gubler**[b], **Lucia Cevidanes**[c], and **André Mol**[d]

[a] Professor, Department of Diagnostic Sciences and General Dentistry, School of Dentistry, University of North Carolina, Chapel Hill

[b] Associate professor, Divison of Radiology, Department of Diagnostic Sciences, Nova Southeastern University, College of Dental Medicine, Miami, Fla

[c] Assistant professor, Department of Orthodontics, School of Dentistry, University of North Carolina, Chapel Hill

[d] Assistant professor, Department of Diagnostic Sciences and General Dentistry, School of Dentistry, University of North Carolina, Chapel Hill

Abstract

Introduction—In this study, we compared the precision of landmark identification using displays of multi-planar cone-beam computed tomographic (CBCT) volumes and conventional lateral cephalograms (Ceph).

Methods—Twenty presurgical orthodontic patients were radiographed with conventional Ceph and CBCT techniques. Five observers plotted 24 landmarks using computer displays of multi-planer reconstruction (MPR) CBCT and Ceph views during separate sessions. Absolute differences between each observer's plot and the mean of all observers were averaged as 1 measure of variability (ODM). The absolute difference of each observer from any other observer was averaged as a second measure of variability (DEO). ANOVA and paired *t* tests were used to analyze variability differences.

Results—Radiographic modality and landmark were significant at $P < 0.0001$ for DEO and ODM calculations. DEO calculations of observer variability were consistently greater than ODM. The overall correlation of 1920 paired ODM and DEO measurements was excellent at 0.972. All bilateral landmarks had increased precision when identified in the MPR views. Mediolateral variability was statistically greater than anteroposterior or caudal-cranial variability for 5 landmarks in the MPR views.

Conclusions—The MPR displays of CBCT volume images provide generally more precise identification of traditional cephalometric landmarks. More precise location of condylion, gonion, and orbitale overcomes the problem of superimposition of these bilateral landmarks seen in Ceph. Greater variability of certain landmarks in the mediolateral direction is probably related to inadequate definition of the landmarks in the third dimension.

Landmark-based analysis with linear and angular measurements is the most common method of cephalometric analysis for growth and treatment assessments. Recent studies have shown that measurements from 2-dimensional (2D) cephalograms generated from cone-beam computed tomography (CBCT) are comparable with measurements obtained directly from dry

Reprint requests to: John B. Ludlow, 1008 Tarson Hall, University of North Carolina School of Dentistry, Chapel Hill, NC 27599-7450; jbl@email.unc.edu.

The authors report no commercial, proprietary, or financial interest in the products or companies described in this article.

skulls[1] and from conventional cephalograms of patients.[2] A preliminary step in establishing CBCT imaging as a common orthodontic diagnostic approach is to assess the precision of the identification of landmarks routinely used for orthodontic diagnosis. This has been extensively done for 2D cephalometric measurements, but the precision of identifying common cephalometric landmarks in 2D cephalograms has not yet been compared with identification of the same landmarks in 3-dimensional (3D) CBCT images of orthodontic patients.[3,4] Many 2D cephalometric analyses have been proposed since the introduction of the cephalostat, but the precision of common cephalometric landmarks is important if the transition in methodologies is to occur in both practice and research settings to allow comparisons with existing databases.

Problems associated with conventional cephalograms—eg, errors in patient position, differential magnification of bilateral structures, and superimposition of craniofacial structures—complicate precise localization of cephalometric landmarks.[5,6] Landmark localization is further complicated by significant asymmetry as in patients with craniofacial syndromes. In spite of these issues, lateral cephalograms have been used for craniofacial and orthognathic surgical planning and monitoring because of the ease of reproducibility and low cost.[7]

Three-dimensional computed tomography (CT) avoids anatomic superimposition and problems caused by magnification and permits evaluation of the craniofacial structures from unobstructed perspectives and with less distortion than plane film views.[8] Unfortunately, this technique suffers from relatively high cost and high radiation dose.[9] In the past decade, CBCT devices have been developed for head and neck imaging. The characteristics of these dedicated maxillofacial devices, including reduced cost and dose, are well suited for imaging the craniofacial area.[10] Some CBCT scanners can collect complete volume data during a half rotation around the patient in only 9 seconds. These scanners use cone- or pyramid-shaped beam geometry, which permits more efficient utilization of x-ray photons compared with the thin fan-shaped geometries that are characteristic of many medical CT devices. CBCT systems offer images with high spatial resolution both longitudinally and axially because of an isotropic voxel matrix. This produces submillimeter resolution from 0.4 to 0.125 mm.[11,12] Some CBCT scanners provide large image fields (9–12 in), which allow 3D reconstruction and visualization of the full maxillofacial region. The value of CBCT imaging in implant planning, surgical assessment of pathology, temporomandibular joint assessment, and preoperative and postoperative assessment of craniofacial structures has been reported.[13–15] For these reasons, 3D CT is increasingly used in maxillofacial surgery and orthodontics for a variety of clinical and research purposes.[16]

Traditionally, lateral and frontal cephalometric radiographs have been used to determine craniofacial discrepancies and deformities, with the analysis based on a series of cephalometric points. Localization of these points can be difficult because of superimposing anatomic structures and differential magnification of bilateralstructures; this results in image distortion.[17] Inaccuracy and poor precision in reproducing cephalometric points with conventional cephalograms are well documented.[4–6,18] The use of CBCT instead of conventional cephalograms is an alternative method for the assessment of craniofacial relationships of orthodontic and surgical patients. However, few studies have compared the accuracy of CBCT and conventional cephalograms.

In this study, we attempted to determine whether correlated axial, frontal, and sagittal multiplanar reconstruction (MPR) images derived from CBCT image volumes provide more precise location of landmarks than conventional cephalometric radiographs. The specific aim was to test the null hypothesis that the precision of landmark identification is not different for CBCT MPR displays and conventional cephalograms in a sample of presurgical orthodontic patients.

MATERIAL AND METHODS

With Institutional Review Board approval, 20 presurgical orthodontic patients at the University of North Carolina School of Dentistry were radiographed by using lateral cephalometric and CBCT techniques. Conventional cephalograms were acquired with the patient in natural head position, stabilized by ear rods. A standardized source to midsagittal plane distance of 152.4 cm (5 feet) and a detector to midsagittal distance of 11.5 cm provided image magnification of 7.5% for midsagittal structures. Photostimulable phosphor plate cassettes were used for image capture. The plates were scanned and digitized at 300 dpi and 16 bits (Digora PCT, Soredex, Milwaukee, Wisc) and saved in a lossless (JPG 100) format. The images were imported into Dolphin 2D (version 10, Dolphin Imaging & Management Systems, Chatsworth, Calif) for viewing.

CBCT volumes were acquired with a NewTom 3G (QR-NIM s.r.l., Verona, Italy). A 12-in receptor field was used, and the patients were positioned to include the soft-tissue contours of the face in the image volume. The “large field” and “high resolution” options were selected for primary image reconstruction. The secondary study data were generated with 0.4-mm axial slice thicknesses and isotropic voxels. The axial images were exported in DICOM format and imported in Dolphin 3D (version 10.5, Dolphin Imaging & Management Systems) for subsequent processing and display.

To obtain diagnostically suitable images for landmark identification, 3 steps were required to process the image volume. First, segmentation was performed for the soft and hard tissues when manipulation of the histogram limits the data that are displayed. An attempt was made to reduce noise without reducing actual soft-tissue or osseous anatomy. Although natural head position has been described as ideal for lateral cephalogram acquisition, the extracranial references (midsagittal ruler, chain) of natural head position are not included in CBCT volumes.[19] For this reason, we used intracranial reference planes to approximate the orientation of a patient in a conventional cephalometric image after segmentation of the data. By using the coronal view, the volume was rotated mediolaterally until the transporionic line of the data was oriented horizontally (Fig 1, *A*). By using the axial view, the volume was rotated until the midsagittal plane of the data was oriented vertically (Fig 1, *B*). In the sagittal view, the volume was rotated anteroposteriorly until the Frankfort plane of the data was oriented horizontally (Fig 1, *C*).

After segmentation and orientation of the image volume, the data were displayed in a 4-panel window containing sagittal, axial, and frontal MPR views as well as a user-selectable surface rendering of bone, soft tissue, or combined bone and soft tissue depicted in a lateral projection (Fig 2). Conventional cephalograms and MPR views were displayed on separate computer workstations for observer identification of cephalometric landmarks.

The landmarks listed in Table I were chosen to assess observer precision in this study. These landmarks included both vertical and anteroposterior components of the craniofacial structures. The landmarks represent midsagittal and bilateral anatomic features with differing degrees of identification difficulty.

Conventional images were calibrated before landmark identification by each observer. This was done by using the computer mouse to click on points at 0 and 40 mm of the radiographic image of an aluminum ruler included in the midsagittal plane of each image. The dimension for this measured distance was input as 40.0 mm to correct for anatomic magnification at the midsagittal plane and to establish the metric for the subsequent measurement matrix that the software would use to record the mouse-click positions for landmarks. The 2D measurement matrix was established with a vertex at the upper left corner of the image. The horizontal

orientation of the matrix was established with a second reference point at the upper right corner of the image.

Five observers participated in this study. Two were experienced oral and maxillofacial radiologists (J.B.L. and A.M.); one was a third-year radiology resident; one was an experienced orthodontist (L.C.); and one was a second-year orthodontic resident. Before the viewing sessions, each observer received written and verbal instructions and was trained in the use of the 2 modalities with a set of 10 CBCT scans and conventional cephalograms not included in this study. The observers viewed the modalities separately in alternating order, reviewing half of the subjects with 1 modality and then half of the subjects with the other modality. The 4 observation sessions for each observer were spread over 2 weeks. The observers were permitted to use enhancement tools such as magnification, brightness, and contrast to improve the visualization of the landmarks. After the observers digitized all landmarks, the landmark coordinates were exported into Excel (Microsoft, Red-mond, Wash) and saved for subsequent assessment of precision.

Statistical analysis

Precision was calculated for 24 landmarks, 2 modalities, and 20 subjects with 2 formulas. The first formula calculated average observer difference from the mean (ODM). First, the mean anteroposterior (AP), caudal-cranial (CC), and, for the MPR views, mediolateral (ML) coordinates were calculated from the 5 observers' location of the same landmark on the same subject and with the same modality. Then the absolute value of the difference of each observer's point location from the mean was calculated for the AP, CC, and ML directions. Finally, the average of all observers' absolute differences from the mean was determined for each direction and the average of AP and CC directions for subsequent paired comparisons of the 2 modalities. The second formula for determining observer variability used the average of all combinations of the absolute value of the difference of 1 observer from another, or the difference for every observer (DEO).

Analysis of variance (ANOVA) was computed for ODM or DEO as outcome variables. Modality, landmark, and axis of measurement (AP, CC) as principal effects as well as all first-order interactions of these effects were included in the ANOVA model. An alpha of 0.05 was established as the level for statistical significance. Paired *t* tests were also used to assess the 2 calculations of variability for each landmark. Because many landmarks and 2 modalities were investigated, the risk of a type II error was increased; therefore, the Bonferroni adjustment for multiple comparisons ($2 \times 24 = 48$) was applied, and a *P* threshold of 0.001 for an alpha level of 0.05 was calculated ($\alpha/n = 0.05/48$). An additional ANOVA was performed on MPR data to compare variability among the 3 axes (AP, CC, and ML).

RESULTS

Table II shows the ANOVA for ODM and DEO by landmark, modality, and axis direction. Every effect and the primary interactions between effects show a statistically significant difference at the $P < 0.05$ level. DEO calculations of observer variability were consistently greater than ODM. Overall correlation of 1920 paired ODM and DEO measurements was excellent at 0.977. Table III presents paired *t* tests of ODM variation difference between MPR and conventional cephalograms for each landmark. Of 24 landmarks, 13 had statistically less variability in at least 1 direction of measurement (AP or CC) in the MPR views.

Figure 3 shows averaged AP and CC DEO variations sorted by increasing variability of conventional cephalometric landmarks. Variability was consistently greater in the conventional views. Average DEO variability was lowest for sella (1.1 mm) and highest for gonion (3.0 mm)

in the conventional cephalogram views, and lowest for sella (0.7 mm) and highest for soft-tissue pogonion (2.6 mm) in the MPR views. Figure 4 shows that, subject by subject, conventional cephalometric images had greater variability than MPR views in 13 subjects, approximately equal variability in 6 subjects, and lower variability in 1 subject ($P = 0.0006$).

Table IV compares DEO variability by the 3 directional axes in the MPR views. *P* values were computed for each landmark with ANOVA. Statistically greater variation in the AP dimension was seen for anterior nasal spine. Greater variation in the CC direction was seen for A-point, pogonion, porion, soft-tissue A-point, and soft-tissue pogonion. Significantly greater variation in the ML direction was seen for condylion, mandibular incisor tip, maxillary incisor tip, orbitale, and porion.

DISCUSSION

Landmark identification with MPR views was accomplished with statistically less variability than conventional cephalograms. Rejection of the null hypothesis of no difference between conventional cephalometric imaging and MPR views was not surprising because of our initial supposition that increased variability is a function of structure noise from the superimposition of bilateral structures in conventional cephalograms. This explanation is supported by the finding that the bilateral landmarks condylion, gonion, and orbitale were each statistically less variable in the MPR views. These findings are consistent with a previous study demonstrating that overlapping of bilateral structures in conventional cephalograms resulted in observer selection of a point intermediate between the 2 outlines, introducing errors in landmark localization.[20]

Less intuitive is that statistically significant differences were found for several midsagittal structures. Thirteen of 23 landmarks (Table III) were significantly more precisely located in the MPR views than in the conventional cephalograms.

When variability of MPR landmark localization was compared for the AP, CC, and ML planes, significantly greater variability was found for 1 landmark in the AP direction, 4 landmarks in the CC direction, and 5 landmarks in the ML direction. Landmarks incorporating mediolaterally oriented linear features have more potential for greater variability when the linear aspect of the feature is horizontal. Examples of this are the incisal edges of the maxillary and mandibular incisors. ML variability could be reduced by stipulating a specific ML position for the point, such as the center of the tooth. Although definitionally less ambiguous, the inferior orbital margin might have also challenged observers with a relatively flat ML linear form in some subjects. A saddle-shaped or ML flat condyle has a similar challenge for observers.

Porion has both ML and CC complexity in the MPR views. Some observers localized this structure in the soft tissues of the ear canal, but others localized it on a bone/soft-tissue margin. Figure 5, *B*, illustrates the possible positions for locating porion, depending on whether bony or soft-tissue contours are used and whether most superior or lateral positions for this feature are chosen. Figure 5, *A*, illustrates the difficulty in visualizing anatomic porion in a conventional cephalometric example. Use of an alternative mechanical porion, while increasing localization precision, could place this landmark more than 1 cm from its anatomic position.

Figure 4 shows that conventional cephalometric imaging was less variable than MPR in only 1 of 20 subjects. When we assessed the volume of this patient for subjective image quality, the soft-tissue contour was made somewhat equivocal because of image noise. This type of noise can be increased by minor patient motion such as swallowing during image acquisition.

Two techniques for controlling AP head rotation were used in this study: Frankfort horizontal in the MPR views and natural head position in the conventional cephalometric views. Differences in rotation of the midsagittal plane should have little impact on landmark identification because this is analogous to small rotations of the monitor or the observer's head while viewing an image. Differences in Frankfort plane orientation because of head position make a small difference in the distribution of the x and y components of landmark variation that is measured in the measurement matrix; however, these differences are estimated to be less than 1.5% for angular changes up to 10° in the Frankfort plane (cosine 10° = 0.985).

Development of methods for landmark location in MPR views requires modification of 2D landmark definitions. In 2D cephalograms, many landmarks are defined as the uppermost or lowermost point of structures, and the third dimension of the landmark location is not defined. Additionally, a point on the edge of a structure in a lateral cephalogram might not correspond to the same point in the coronal cephalogram, because of the potential for patient rotation around the ear rods of the cephalostat and the different x-ray beam projections that result from this rotation. Whereas the absence of spatial correspondence between 2D views is a problem in 2D cephalograms, 3D coordinate points in MPR views corresponded more closely to anatomic truth and allowed pinpoint locations in the same anatomic locus in correlated views.[21]

The sources of error in landmark identification in this study could be 3-fold. First, in the MPR views, the landmarks require definitions for ML localization in addition to the traditional AP and CC directions. Second, some landmarks can be easily identified in 1 or 2 planes of the space, but landmark identification in the third plane might be difficult. Observers in this study tended to locate the landmark in the planes of easy identification, disregarding the plane of difficult visualization. Third, selection of the best slice for landmark location in each direction (AP, CC, and ML) requires time, calibration training, and careful assessment. Three-dimensional landmark identification is more time-consuming than conventional 2D cephalogram tracing because it requires identifying landmarks in coronal, sagittal, and axial views, and double-checking the visualization in the 3 planes of space.[22]

Although the assessment of landmark identification reliability has been extensive for cephalometric measurements, little has been published for medical maxillofacial CT imaging and still less for CBCT images.[23] In a comparison of cephalometric and spiral CT for reliability of traditional cephalometric landmarks with skulls, 9 landmarks had significantly less interrater variation with the lateral cephalometric method than in the 3D CT method. A reversal in trends in this study with significantly lower interobserver variation for 13 of 24 landmarks in the CBCT MPR views compared with conventional cephalograms might be related to the larger 2-mm acquisition slices used for the 0.4-mm voxel reconstruction in the study by Kragskov et al.[24]

Several factors must be considered in choosing a radiographic examination, including the probability of obtaining the diagnostic information that is sought from it, its cost, and its risks. These must be weighed against the same factors for alternate diagnostic procedures and the value of the information that is sought and the risks and costs of inadequate diagnosis. Standard orthodontic diagnosis often includes panoramic, lateral cephalometric, and PA cephalometric radiography. The estimated risk from these 3 examinations according to the 2007 recommendations for calculating the effective dose is between 25 and 35 μSv.[25] Alternate CBCT doses from 1 large field of view scan that is useful for complete orthodontic diagnosis range from 68 to 1073 μSv.[26] The excess risk, depending on the radiographic device, is equivalent to a few days to several weeks of average per capita background dose in the United States. If the diagnostic information from the CBCT scan improves treatment results, shortens treatment time, or reduces treatment cost, the increased risk might be worthwhile. Without

such a benefit, the technique cannot be recommended. More study of the impact of CBCT diagnostics on patient treatment is needed.

CONCLUSIONS

1. Observer identification of cephalometric landmarks was significantly more precise with MPR views of CBCT volumes than with conventional lateral cephalograms, even when using traditional 2D definitions for these landmarks.
2. The MPR views provide significantly more precise location of condylion, gonion, and orbitale, overcoming the problem of superimposition of these bilateral landmarks seen in conventional cephalograms.
3. Increased variability of certain landmarks in the ML direction is most likely related to inadequate definition of landmarks in the third dimension.
4. Revised definitions of 2D cephalometric landmarks will be needed to take full advantage of the increased precision with MPR displays of image volumes.

Acknowledgments

Supported by grant NDCR DE 00521526.

References

1. Kumar V, Ludlow JB, Mol A, Cevidanes L. Comparison of conventional and cone beam CT synthesized cephalograms. Dentomaxillofac Radiol 2007;36:263–9. [PubMed: 17586852]
2. Kumar V, Ludlow J, Cevidanes LHS, Mol A. In vivo comparison of conventional and cone beam CT synthesized cephalograms. Angle Orthod 2008;78:873–9. [PubMed: 18298214]
3. Halazonetis DJ. From 2-dimensional cephalograms to 3-dimensional computed tomography scans. Am J Orthod Dentofacial Orthop 2005;127:627–37. [PubMed: 15877045]
4. Baumrind S, Frantz RC. The reliability of head film measurements. 1. Landmark identification. Am J Orthod 1971;60:111–27. [PubMed: 5283996]
5. Midtgard J, Bjork G, Linder-Aronson S. Reproducibility of cephalometric landmarks and errors of measurements of cephalometric cranial distances. Angle Orthod 1974;44:56–61. [PubMed: 4520951]
6. Houston WJ. The analysis of errors in orthodontic measurements. Am J Orthod 1983;83:382–90. [PubMed: 6573846]
7. Por YC, Barcelo CR, Sng K, Genecov D, Salyer K. A novel method for measuring and monitoring monobloc distraction osteogenesis using three dimensional computed tomography rendered images with the “biporion-dorsum sellae” plane. Part I: precision and reproducibility. J Craniofac Surg 2005;16:430–5. [PubMed: 15915109]
8. Papadopoulos M, Jannowitz C, Boettcher P, Henke J, Stolla R, Zeilhofer H, et al. Three-dimensional fetal cephalometry: an evaluation of the reliability of cephalometric measurements based on three-dimensional CT reconstructions and on dry skulls of sheep fetuses. J Craniomaxillofac Surg 2005;33:229–37. [PubMed: 15978824]
9. Ngan DC, Kharbanda OP, Geenty JP, Darendeliler MA. Comparison of radiation levels from computed tomography and conventional dental radiographs. Aust Orthod J 2003;19:67–75. [PubMed: 14703331]
10. Ludlow JB, Brooks SL, Davies-Ludlow LE, Howerton B. Dosimetry of 3 CBCT units for oral and maxillofacial radiology. Dentomaxillofac Radiol 2006;35:219–26. [PubMed: 16798915]
11. Yajima A, Otonari-Yamamoto M, Sano T, Hayakawa Y, Otonari T, Tanabe K, et al. Cone-beam CT (CB throne) applied to dentomaxillofacial region. Bull Tokyo Dent Coll 2006;47:133–41. [PubMed: 17344621]
12. Scarfe W, Farman A, Sukovic P. Clinical applications of cone-beam computed tomography in dental practice. J Can Dent Assoc 2006;72:75–80. [PubMed: 16480609]

13. Honda K, Arai Y, Kashima M, Takano Y, Sawada K, Ejima K, et al. Evaluation of the usefulness of the limited cone-beam CT (3DX) in the assessment of the thickness of the roof of the glenoid fossa of the temporomandibular joint. Dentomaxillofac Radiol 2004;33:391–5. [PubMed: 15665233]
14. Honda K, Matumoto K, Kashima M, Takano Y, Kawashima S, Arai Y. Single air contrast arthrography for temporomandibular joint disorder using limited cone beam computed tomography for dental use. Dentomaxillofac Radiol 2004;33:271–3. [PubMed: 15533984]
15. Tsiklakis K, Syriopoulos K, Stamatakis HC. Radiographic examination of the temporomandibular joint using cone beam computed tomography. Dentomaxillofac Radiol 2004;33:196–201. [PubMed: 15371321]
16. Kitaura H, Yonetsu K, Kitamori H, Kobayashi K, Nakamura T. Standardization of 3-D CT measurements for length and angles by matrix transformation in the 3-D coordinate system. Cleft Palate Craniofac J 2000;37:349–56. [PubMed: 10912713]
17. Bergersen EO. Enlargement and distortion in cephalometric radiography: compensation tables for linear measurements. Angle Orthod 1980;50:230–44. [PubMed: 6931505]
18. Kantor ML, Phillips CL, Proffit WR. Subtraction radiography to assess reproducibility of patient positioning in cephalometrics. Am J Orthod Dentofacial Orthop 1993;104:350–4. [PubMed: 8213656]
19. Lundström A, Lundström F, Lebret LM, Moorrees CF. Natural head position and natural head orientation: basic considerations in cephalometric analysis and research. Eur J Orthod 1995;17:111–20. [PubMed: 7781719]
20. Hurst CA, Eppley BL, Havlik RJ, Sadove AM. Surgical cephalometrics: applications and developments. Plast Reconstr Surg 2007;120:92e–104e.
21. Katsumata A, Fujishita M, Maeda M, Ariji Y, Ariji E, Langlais RP. 3D-CT evaluation of facial asymmetry. Oral Surg Oral Med Oral Pathol Oral Radiol Endod 2005;99:212–20. [PubMed: 15660095]
22. Oliveira AEF, Cevidanes LHS, Phillips C, Motta A, Burke B, Tyndall D. Observer reliability of three-dimensional cephalometric landmark identification on cone-beam computed tomography. Oral Surg Oral Med Oral Pathol Oral Radiol Endod 2000;107:256–65. [PubMed: 18718796]
23. Lou L, Lagravere MO, Compton S, Major PW, Flores-Mir C. Accuracy of measurements and reliability of landmark identification with computed tomography (CT) techniques in the maxillofacial area: a systematic review. Oral Surg Oral Med Oral Pathol Oral Radiol Endod 2007;104:402–11. [PubMed: 17709072]
24. Kragskov J, Bosch C, Gyldensted C, Sindet-Pedersen S. Comparison of the reliability of craniofacial anatomic landmarks based on cephalometric radiographs and three-dimensional CT scans. Cleft Palate Craniofac J 1997;34:111–6. [PubMed: 9138504]
25. Ludlow JB, Davies-Ludlow LE, White SC. Patient risk related to common dental radiographic examinations: the impact of 2007 International Commission on Radiological Protection recommendations regarding dose calculation. J Am Dent Assoc 2008;139:1237–43. [PubMed: 18762634]
26. Ludlow JB, Ivanovic M. Comparative dosimetry of dental CBCT devices and 64 row CT for oral and maxillofacial radiology. Oral Surg Oral Med Oral Pathol Oral Radiol Endod 2008;106:930–8.

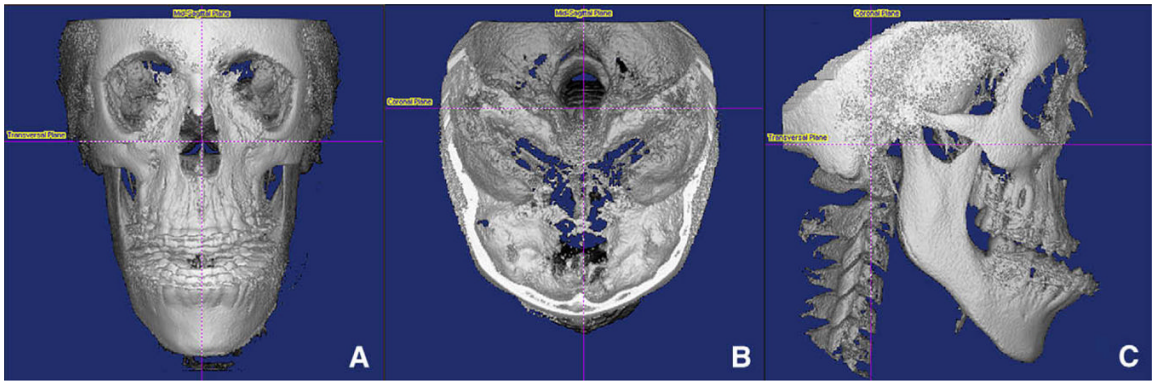

Fig 1.

Orientation of the CBCT volume before generation of the MPR radiographic views: **A,** vertical orientation of the midsagittal plane; **B,** rotation of the transporionic axis to establish the coronal plane; **C,** rotation of the Frankfort plane to the horizontal orientation.

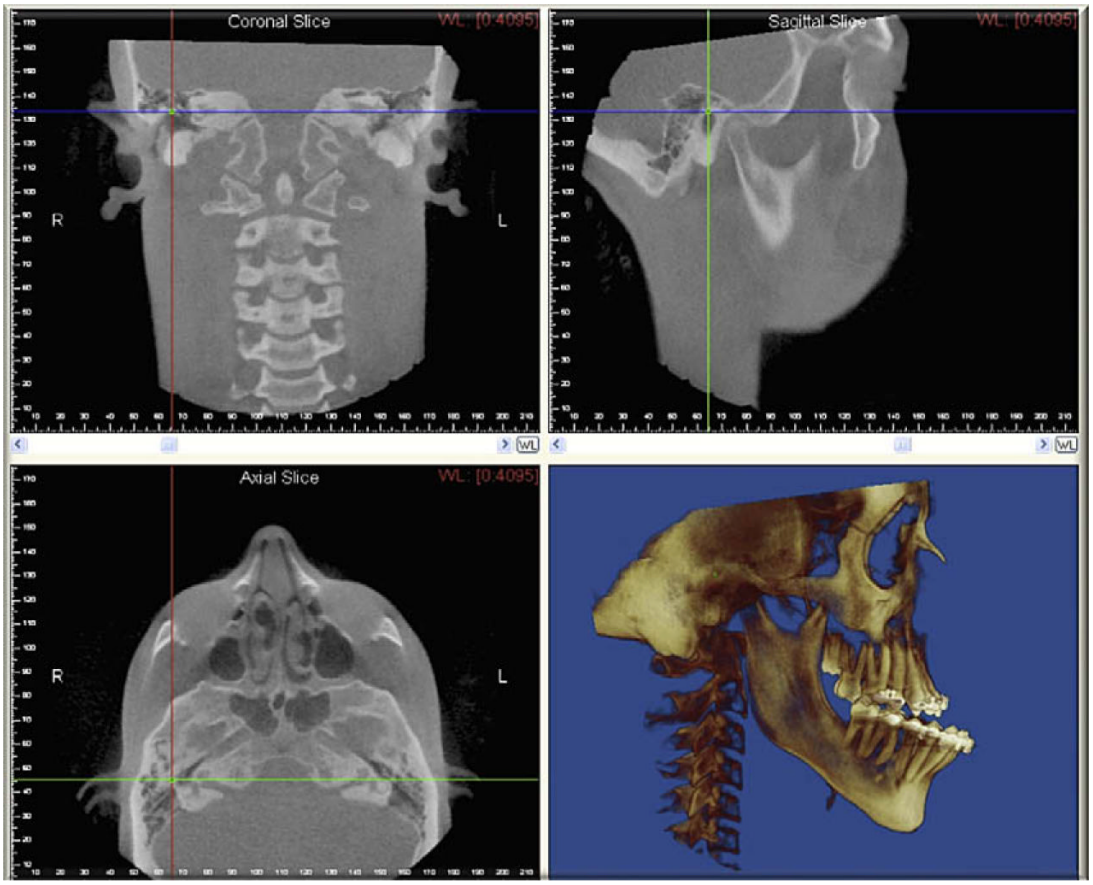

Fig 2.
Landmark location window displaying coronal, sagittal, and axial MPR views with surface-rendered skeletal volume.

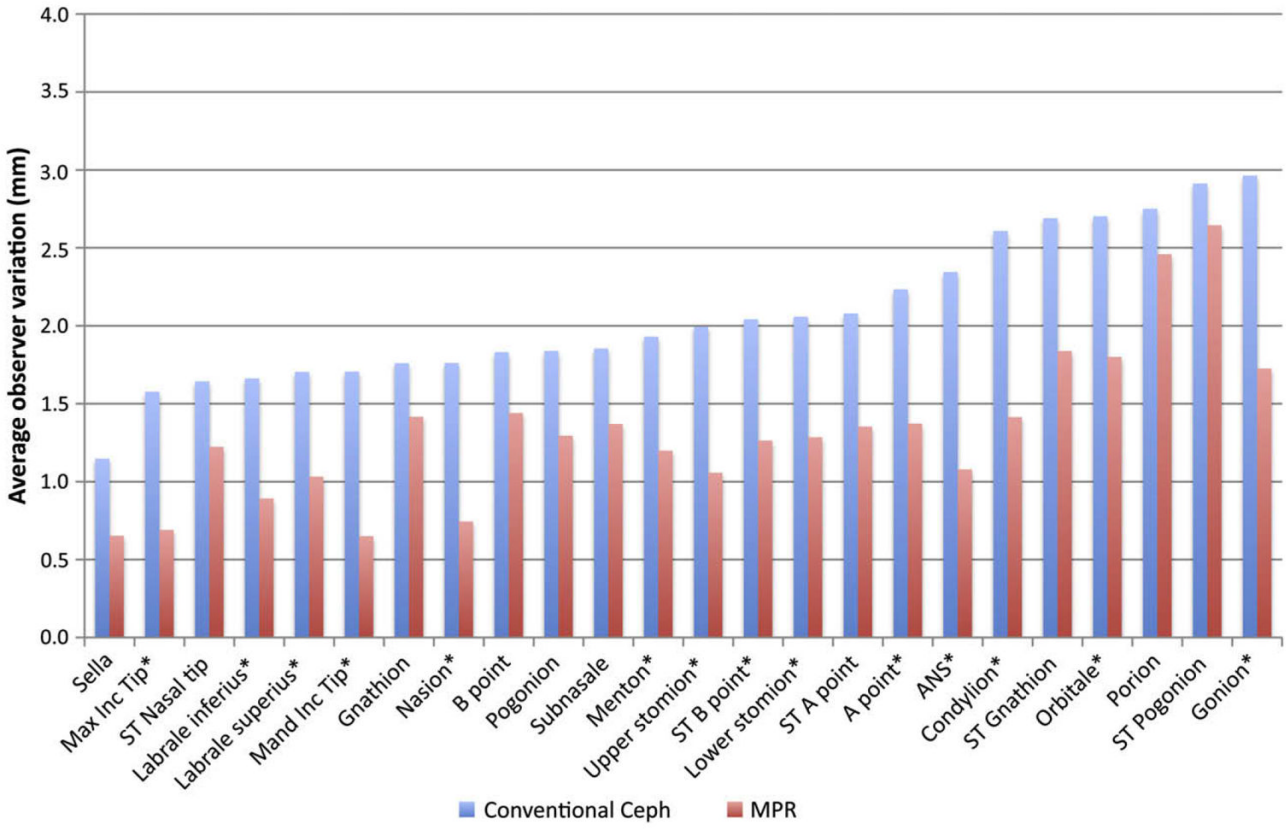

Fig 3.

Average of AP and CC DEO variation by landmark for conventional cephalometric and MPR views. *Significant at $P = 0.001$.

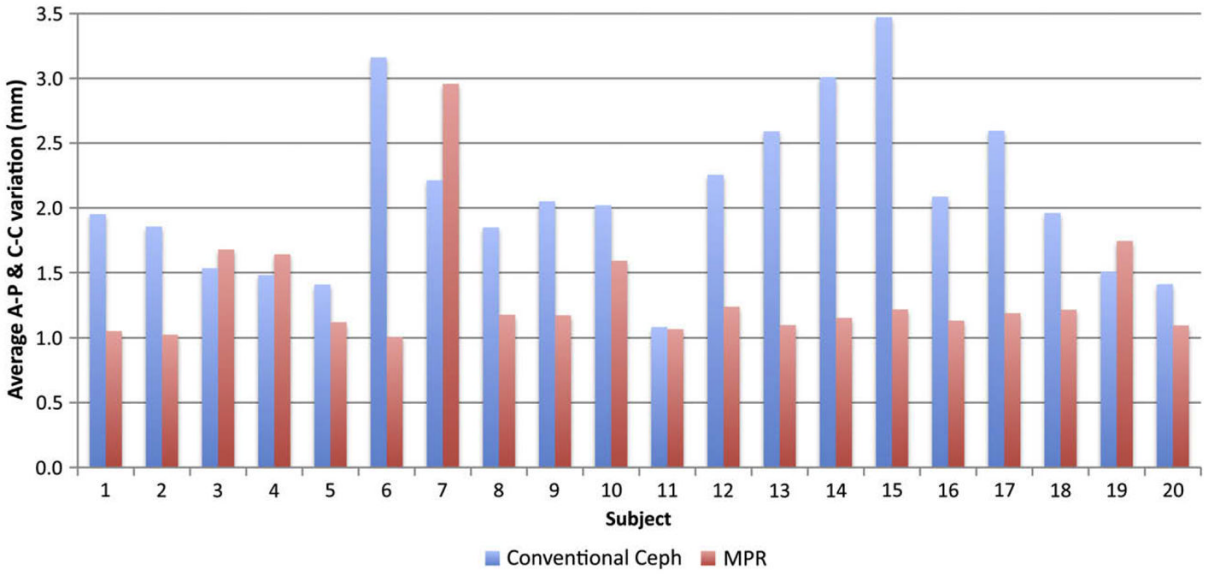

Fig 4.

Average of AP and CC DEO variations for all landmarks by subject for conventional cephalometric and MPR views.

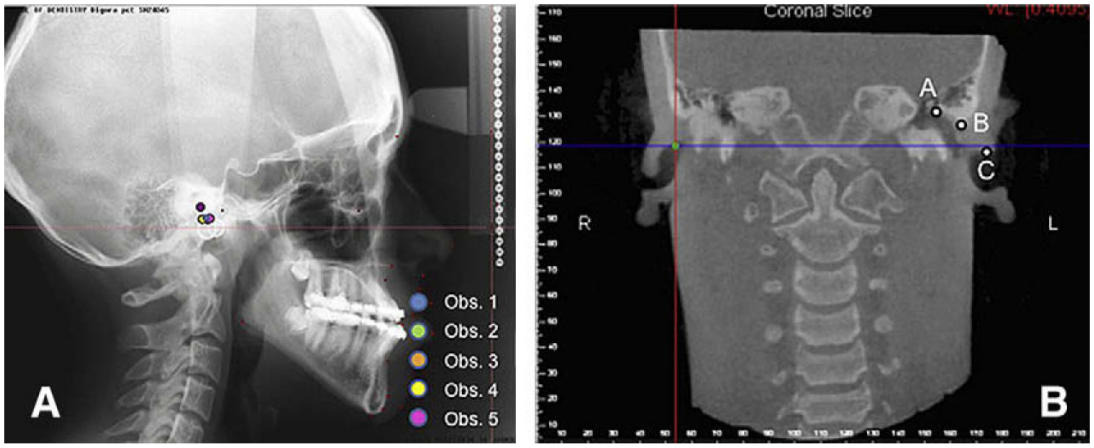

Fig 5.

A, Conventional cephalogram showing observer variability in porion identification. Observers 1, 3, 4, and 5 appeared to be using the mechanical porion definition for their location, but observer 2 attempted to locate the anatomic porion. **B,** Coronal slice from the MPR view illustrating different ML and CC positions that might be used in identifying porion: *A*, highest bony segment of the auditory canal; *B*, most lateral segment of the bony auditory canal; *C*, most external segment of the soft-tissue component of the auditory canal; this corresponds most closely to the CC position of mechanical porion seen in the conventional cephalogram.

Table I

Landmark definitions

Landmark	Definition
A-point	Deepest point of the curve of the maxilla, between anterior nasal spine and the dental alveolus
ANS	Tip of the anterior nasal spine
B-point	Most posterior point in the concavity along the anterior border of the symphysis
Condylion	Most posterior superior point of the right condyle
Gnathion	Midpoint between the most anterior and inferior point on the bony chin
Gonion	Location depends of the analysis: **1** the most convex point along the inferior border of the right ramus **2** the most convex point where the posterior inferior curve of the right ramus and ascending ramus meet
Labrale inferius	Most anterior point on the curve of the lower lip
Labrale superius	Most anterior point on the curve of the upper lip
Lower stomion	Most superior point on the curve of the lower lip
Mand inc tip	Tip of the mandibular right central incisor
Max inc tip	Incisal tip of the maxillary right central incisor
Menton	Most inferior point of the symphysis
Nasion	Intersection of the internasal suture with the nasofrontal suture in the midsagittal plane
Orbitale	Lowest point of the floor of the right orbit, the most inferior point of the external border of the orbital cavity
Pogonion	Most anterior point on the midsagittal symphysis
Porion	Most superior point of the right external auditory meatus
Sella	Center of the pituitary fossa of the sphenoid bone
Soft-tissue A-point	Most concave point between subnasale and the anterior point of the upper lip
Soft-tissue B-point	Most concave point between the lower lip and the soft-tissue chin
Soft-tissue gnathion	Midpoint between the most anterior and inferior points of the soft-tissue chin in the midsagittal plane
Soft-tissue pogonion	Point on the anterior curve of the soft-tissue chin
Soft-tissue nasal tip	Pronasale, point of the anterior curve of the nose
Subnasale	Point where the nose connects to the center of the upper lip
Upper stomion	Most inferior point on the curve of the upper lip

Table II

ANOVA with observer difference from the mean (ODM) or difference of each observer from every other observer (DEO) as outcome variables

		ODM			DEO		
Source	**df**	**Sum of squares**	**F ratio**	***P*** **> F**	**Sum of squares**	**F ratio**	***P*** **> F**
Landmark	23	165.6	16.5	<0.0001	401.1	17.4	<0.0001
Modality	1	156.6	359.8	<0.0001	266.8	266.9	<0.0001
Axis (AP, CC)	1	115.8	266.1	<0.0001	165.9	166.0	<0.0001
Landmark*modality	23	25.0	2.5	0.0001	39.9	1.7	0.0164
Landmark*axis	23	117.8	11.8	<0.0001	300.6	13.1	<0.0001
Modality*axis	1	3.3	7.6	0.0058	29.8	29.8	<0.0001

Table III

Paired *t* test comparisons of MPR and conventional cephalograms ODM variability by landmark

	AP			CC			Averaged AP and CC		
ODM Landmark	**Conventional**	**MPR**	***P***	**Conventional**	**MPR**	***P***	**Conventional**	**MPR**	***P***
A-point	1.20	0.22	<0.0001	1.59	1.24	0.0619	1.40	0.73	<0.0001
ANS	1.61	0.56	<0.0001	1.47	0.46	<0.0001	1.54	0.51	<0.0001
B-point	0.77	0.18	<0.0001	1.54	1.45	0.7937	1.16	0.81	0.1014
Condylion	1.40	0.94	0.0052	1.89	0.64	<0.0001	1.65	0.79	<0.0001
Gnathion	0.80	0.29	0.0025	1.46	1.17	0.4500	1.13	0.73	0.0897
Gonion	1.51	0.67	<0.0001	2.19	1.11	<0.0001	1.85	0.89	<0.0001
Labrale inferius	0.78	0.30	0.0040	1.33	0.70	0.0006	1.06	0.50	<0.0001
Labrale superius	0.80	0.38	0.0048	1.38	0.89	0.0086	1.09	0.63	0.0021
Lower stomion	1.36	0.79	0.0001	1.27	0.62	0.0048	1.32	0.71	<0.0001
Mand inc tip	0.85	0.39	<0.0001	1.35	0.44	0.0002	1.10	0.42	<0.0001
Max inc tip	0.72	0.33	0.0018	1.37	0.48	0.0006	1.05	0.41	0.0001
Menton	1.07	0.33	0.0002	1.45	0.47	0.0002	1.26	0.40	<0.0001
Nasion	0.75	0.32	0.0053	1.59	0.53	<0.0001	1.17	0.42	<0.0001
Orbitale	1.85	0.49	0.2544	1.66	0.49	<0.0001	1.76	1.02	0.0003
Pogonion	0.67	0.35	0.0319	1.67	1.23	0.0241	1.17	0.79	0.0137
Porion	1.06	0.85	0.1542	2.66	2.36	0.3671	1.86	1.60	0.1717
Sella	0.45	0.38	0.6044	1.14	0.40	0.0019	0.80	0.39	0.0027
Soft-tissue A-point	0.80	0.35	0.0141	1.79	1.28	0.0095	1.30	0.81	0.0018
Soft-tissue B-point	0.96	0.16	<0.0001	1.59	1.05	0.0108	1.28	0.60	<0.0001
Soft-tissue gnathion	1.55	1.00	0.0475	1.88	1.25	0.0079	1.72	1.12	0.0050
Soft-tissue nasal tip	0.78	0.53	0.2110	1.31	0.91	0.0626	1.05	0.72	0.0788
Soft-tissue pogonion	1.13	0.86	0.2497	2.53	2.60	0.8353	1.83	1.73	0.6895
Subnasale	1.03	0.96	0.7303	1.33	0.80	0.0229	1.18	0.88	0.1022
Upper stomion	1.18	0.72	0.0212	1.43	0.58	0.0007	1.31	0.65	0.0003
Average	1.05	0.51		1.62	0.96		1.33	0.76	

Bonferroni adjustment = .05/48 = .001.

Table IV

Comparison of landmark identification DEO variability by AP, CC, and ML directions of the MPR views

	MPR			
DEO Landmark	**AP**	**CC**	**ML**	***P***
A-point	0.74	2.01	0.68	<0.0001
ANS	1.43	0.73	0.66	0.0001
B-point	0.69	2.19	1.32	0.0036
Condylion	1.82	1.01	2.55	<0.0001
Gnathion	1.04	1.80	1.40	0.2089
Gonion	1.71	1.75	1.22	0.1393
Labrale inferius	0.65	1.14	1.11	0.0828
Labrale superius	0.66	1.41	0.99	0.0056
Lower stomion	1.57	1.00	1.11	0.0205
Mand inc tip	0.63	0.67	2.06	<0.0001
Max inc tip	0.62	0.76	1.99	<0.0001
Menton	1.65	0.75	1.43	0.0146
Nasion	0.66	0.83	0.65	0.6016
Orbitale	2.80	0.80	5.76	<0.0001
Pogonion	0.69	1.91	1.35	0.0018
Porion	1.46	3.46	7.14	<0.0001
Sella	0.65	0.66	1.05	0.0807
Soft-tissue A-point	0.78	1.93	0.79	<0.0001
Soft-tissue B-point	0.90	1.63	1.20	0.0949
Soft-tissue gnathion	1.73	1.95	1.44	0.423
Soft-tissue nasal tip	0.98	1.47	0.68	0.0057
Soft-tissue pogonion	1.31	3.98	1.44	<0.0001
Subnasale	1.51	1.23	0.75	0.0485
Upper stomion	1.19	0.93	1.20	0.4621
Average	1.16	1.50	1.67	

Bonferroni adjustment = .05/23 = .0022.